Phase transitions in $Ca_3(BN_2)_2$ and $Sr_3(BN_2)_2$

Marco Häberlen, Jochen Glaser, H.-Jürgen Meyer*

Abteilung für Festkörperchemie und Theoretische Anorganische Chemie, Institut für Anorganische Chemie, Eberhard-Karls-Universität, Auf der Morgenstelle 18, D-72076 Tübingen, Germany

Abstract

α-$Ca_3(BN_2)_2$ crystallizes in the cubic system (space group: $Im\bar{3}m$) with one type of calcium ions disordered over $\frac{7}{8}$ of equivalent ($8c$) positions. An ordered low-temperature phase (β-$Ca_3(BN_2)_2$) was prepared and found to crystallize in the orthorhombic system (space group: $Cmca$) with lattice parameters: $a = 1024.18(2)$ pm, $b = 732.43(2)$ pm, and $c = 2091.60(4)$ pm. Structure refinements on the basis of X-ray powder data have revealed that orthorhombic β-$Ca_3(BN_2)_2$ corresponds to an ordered super-structure of cubic α-$Ca_3(BN_2)_2$. The space group $Cmca$ assigned for β-$Ca_3(BN_2)_2$ is derived from $Im\bar{3}m$ by a group–subgroup relationship.

DSC measurements and temperature-dependent in situ X-ray powder diffraction studies showed reversible phase transitions between β- and α-$Ca_3(BN_2)_2$ with transition temperatures between 215 and 240 °C.

The structure $Sr_3(BN_2)_2$ was reported isotypic with α-$Ca_3(BN_2)_2$ ($Im\bar{3}m$) with one type of strontium ions being disordered over $\frac{1}{2}$ of equivalent ($2c$) positions. In addition, a primitive ($Pm\bar{3}m$) structure has been reported for $Sr_3(BN_2)_2$. Phase stability studies on $Sr_3(BN_2)_2$ revealed a phase transition between a primitive and a body-centred lattice around 820 °C. The experiments showed that both previously published structures are correct and can be assigned as α-$Sr_3(BN_2)_2$ ($Im\bar{3}m$, high-temperature phase), and β-$Sr_3(BN_2)_2$ ($Pm\bar{3}m$, low-temperature phase).

A comparison of $Ca_3(BN_2)_2$ and $Sr_3(BN_2)_2$ phases reveals that the different types of cation disordering present in both of the cubic α-phases ($Im\bar{3}m$) have a directing influence on the formation of two distinct (orthorhombic and cubic) low-temperature phases.
© 2005 Elsevier Inc. All rights reserved.

Keywords: Alkaline earth; Nitridoborate; Phase transition; Superstructure

1. Introduction

The existence of a linear $(N–B–N)^{3-}$ ion was first considered by Goubeau and Anselment on the basis of infrared measurements performed on $Li_3(BN_2)$, $Ca_3(BN_2)_2$, and $Ba_3(BN_2)_2$ [1]. About 20 years later, this prediction was approved by the crystal structure refinement of $Li_3(BN_2)$ [2]. The first crystal structure of an alkaline earth nitridoborate was published in the nineties for $Sr_3(BN_2)_2$ [3]. Single crystals of $Sr_3(BN_2)_2$ were found to crystallize in the cubic space group $Im\bar{3}m$ with three formula units per unit cell. One of the two crystallographically distinct strontium ions was refined

to be disordered over the $2a$ position with 50% occupancy, and the other one was refined on a fully occupied $8c$ position, which may be described as $Sr \square [Sr_8](BN_2)_6$. This structure opened grounds for the discovery of a series of ordered alkaline-alkaline earth (A-AE) di-nitridoborates with the general formula $A_2AE_8(BN_2)_6$ and the mixed alkaline earth di-nitrido-borates such as $Mg_2Ca_7(BN_2)_6$ (Table 1) with the same space group $Im\bar{3}m$ [4,5].

Subsequent research on alkaline earth $AE_3(BN_2)_2$ compounds with $AE =$ Ca, Sr, Ba has provided additional structural data in the past 10 years [6–9] but also raised some questions concerning the differences in their crystal structures.

α-$Ca_3(BN_2)_2$ was found to be isotypic to $Sr_3(BN_2)_2$, but with a different cation ordering, where one type of

*Corresponding author. Fax: +49 7071295702.

E-mail address: juergen.meyer@uni-tuebingen.de (H.-J. Meyer).

calcium ions fully occupies a 2a position and the other type is disordered over $\frac{7}{8}$ of equivalent 8c positions of $Im\bar{3}m$, according to $Ca_2[Ca_7 \square](BN_2)_6$ (compared to $Sr \square [Sr_8](BN_2)_6$) [3,4]. For $Ca_3(BN_2)_2$ clear evidence has been found for the existence of a phase transition into a low-temperature phase when the compound was slowly cooled below 265 °C [6]. A super-structure related to the high-temperature phase and a distortion of the cubic unit cell was anticipated, but the powder pattern of the supposed low-temperature modification β-$Ca_3(BN_2)_2$ could not be indexed and the structure remained unknown.

For $Sr_3(BN_2)_2$ a second phase was reported to crystallize in the primitive space group $Pm\bar{3}m$, instead

Table 1
Some di-nitridoborates crystallizing with the space group $Im\bar{3}m$

LiCa$_4$(BN$_2$)$_3$	[4]
LiSr$_4$(BN$_2$)$_3$	[4]
LiEu$_4$(BN$_2$)$_3$	[4]
LiBa$_4$(BN$_2$)$_3$	[4]
NaSr$_4$(BN$_2$)$_3$	[4]
NaEu$_4$(BN$_2$)$_3$	[4]
NaBa$_4$(BN$_2$)$_3$	[4]
Mg$_2$Ca$_7$(BN$_2$)$_6$	[5]

of the previously reported space group $Im\bar{3}m$. A phase relationship comparable to the calcium compound was suggested for $Sr_3(BN_2)_2$. But it still was not clear if the first structure reported for $Sr_3(BN_2)_2$ was a high-temperature modification [7]. In addition, the correctness of the body-centred structure was questioned after the structure of $Eu_3(BN_2)_2$ was refined in the primitive space group $Pm\bar{3}m$ [10].

In case of $Ba_3(BN_2)_2$ a cubic structure has been reported, however, a satisfying crystal structure refinement is not yet known. In addition, an orthorhombic modification of $Ba_3(BN_2)_2$ has been reported recently [9]. A structural relationship that would allow a phase transition between the two reported $Ba_3(BN_2)_2$ structures appears more difficult to explain than for the calcium and strontium compounds. These questions about the structure and phase transitions of alkaline earth di-nitridoborates prompted us to reinvestigate the $AE_3(BN_2)_2$ system for $AE =$ Ca and Sr.

Fig. 1(a) displays the structure of the high-temperature modifications of cubic α-$AE_3(BN_2)_2$ compounds with $AE =$ Ca, Sr, in which only nine out of ten cation positions in the unit cell are occupied. As previously mentioned, the cation ordering corresponds to a partially occupied 8c site $\left(\frac{1}{4}, \frac{1}{4}, \frac{1}{4}; \ldots\right)$ for Ca_2
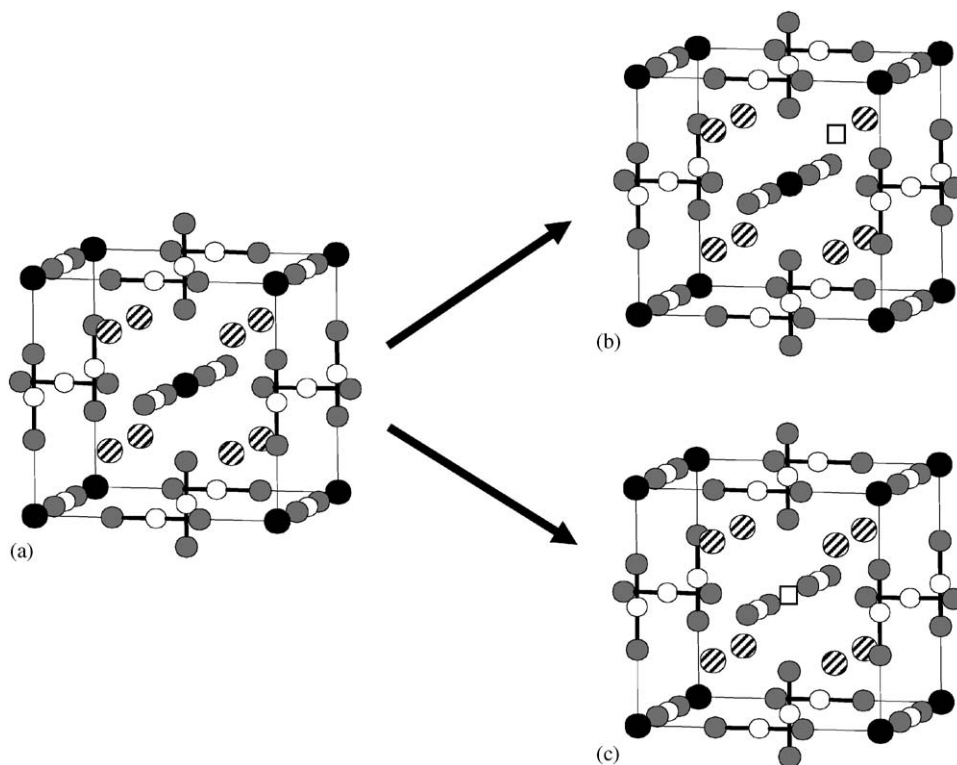

Fig. 1. Real and possible modifications of $AE_3(BN_2)_2$ compounds with AE positions shown as black and hatched spheres. The $(NBN)^{3-}$ ions are shown as three-connected units with white B and dark grey N atoms. (a) Unit cell of the disordered high-temperature modifications of $Ca_3(BN_2)_2$ and $Sr_3(BN_2)_2$ with the space group $Im\bar{3}m$. In $Ca_3(BN_2)_2$ the 8c $\left(\frac{1}{4}, \frac{1}{4}, \frac{1}{4}; \ldots\right)$ site is occupied by $\frac{7}{8}$, and in $Sr_3(BN_2)_2$ the 2a (0,0,0 and $\frac{1}{2}, \frac{1}{2}, \frac{1}{2}$) site is occupied by $\frac{1}{2}$ [3,6]. (b) An archetype structure with a symmetry breaking ordering of Ca ions on 8c positions in the low-temperature modification for $Ca_3(BN_2)_2$. The vacancy is represented by a square. (c) The symmetry retaining ordering of the Sr ions on the former 2a positions leads to the low-temperature phase with the space group $Pm\bar{3}m$. The ordered vacancy is represented by a square.

Table 2
Selected crystallographic details and synthesis conditions of alkaline earth di-nitridoborates

| Compound	Space group	Lattice parameters	Synthesis	Lit.
α-$Ca_3(BN_2)_2$	$Im\bar{3}m$	$a = 732.24(3)$ pm	1197 °C, 1 h cooling rate > 30 °C/min	[6]
β-$Ca_3(BN_2)_2$	$Cmca$	$a = 1024.18(2)$ pm $b = 732.43(2)$ pm $c = 2091.60(4)$ pm	900 °C, 40 h cooling rate < 30 °C/min	[*]
$Sr_3(BN_2)_2$	$Im\bar{3}m$	$a = 765.8(1)$ pm	900 °C, 5 d	[3]
$Sr_3(BN_2)_2$	$Pm\bar{3}m$	$a = 765.5(4)$ pm	800 °C, 20 h	[7]
$Ba_3(BN_2)_2$	$Im\bar{3}m$	$a = 800.44(4)$ pm	927 °C, 4 d	[8]
$Ba_3(BN_2)_2$	$P2_12_12_1$	$a = 424.73(2)$ pm $b = 1105.60(4)$ pm $c = 1475.72(6)$ pm	1027 °C, 3 d	[9]

Starting materials in all cases were the alkaline earth nitride or elements and BN.
[*] Results of this work.

$[Ca_7 \square](BN_2)_6$ and a half-occupied $2a$ site $(0,0,0; \frac{1}{2},\frac{1}{2},\frac{1}{2})$ for $Sr \square [Sr_8](BN_2)_6$. The unit cells at the right side of Fig. 1 display a simple structural model of ordered β-$Ca_3(BN_2)_2$ (b), that would in fact require a super-structure, and the ordered structure of the supposed low-temperature modification β-$Sr_3(BN_2)_2$ (c). Table 2 summarizes structural and experimental results of all $AE_3(BN_2)_2$ modifications.

2. Experimental

Di-nitridoboratate ions readily form when alkaline earth metal is melted together with (layer-type) boron nitride, according to
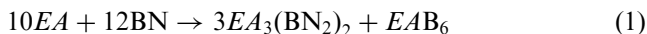
$$10EA + 12BN \rightarrow 3EA_3(BN_2)_2 + EAB_6 \qquad (1)$$
$$EA = Ca, Sr.$$

2.1. Syntheses

Due to the sensitivity of starting materials and products against moisture and air all manipulations of materials were performed under dry Ar atmosphere inside a glove box, or in an airtight glass apparatus. Chemicals were used as purchased (Ca, 99.99%, dendritic, Strem; Sr 99.99%, dendritic, Strem; BN, 99.8%, ABCR, X-ray pure, degassed at 400 °C under dynamic vacuum for 20 h). The alkaline earth nitrides were synthesized from the elements in a continuous flow of nitrogen at 750 °C as reported in [3] and inspected by X-ray powder diffraction.

For the phase transition experiments, we synthesized the low-temperature modifications by reacting alkaline earth nitrides with (layer-type) boron nitride, e.g.,

$$Ca_3N_2 + 2BN \rightarrow Ca_3(BN_2)_2. \qquad (2)$$
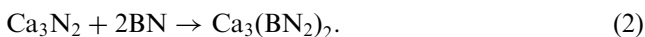
The starting materials were loaded into copper ampoules inside a glove box. In following procedures the ampoules were arc-welded and sealed into evacuated silica tubes. The ampoules were then placed in a chamber furnace, heated up to 950 °C, and held constant for 40 h before lowering the temperature to room temperature within 6 h.

Reaction products contained a white, sometimes light green powder of β-$Ca_3(BN_2)_2$ besides small amounts of CaO and BN impurities. The obtained powders of β-$Sr_3(BN_2)_2$ were dark brown and also contained some SrO and BN impurities. Products typically contained 80–90% alkaline earth di-nitridoborates, according to the X-ray powder diffraction patterns.

2.2. X-ray powder measurements

Powder X-ray diffraction (PXRD) data were collected with an X-ray powder diffractometer STADI-P (germanium monochromator, Cu-$K\alpha_1$; STOE, Darmstadt). The PXRD pattern of β-$Ca_3(BN_2)_2$ was indexed in the orthorhombic system with $a = 1024.18(2)$ pm, $b = 732.43(2)$ pm, and $c = 2091.60(4)$ pm, on the basis of 24 lines. The powder pattern of β-$Sr_3(BN_2)_2$ ($a = 763.8(1)$ pm, $Pm\bar{3}m$, with 16 indexed lines) agreed with the previously reported data [8].

Samples were filled into 0.2 mm capillaries for temperature-dependent X-ray measurement and placed in a high-temperature oven (model 0.65.1, STOE, Darmstadt) for phase transition studies. Useful 2θ ranges for the measurements, that cover relevant reflections for both phases were selected from simulated powder patterns for α- and β-$Ca_3(BN_2)_2$ (Fig. 2), and for α- and β-$Sr_3(BN_2)_2$ (Fig. 3). Heating and the cooling rates were chosen between 10 and 50 °C/min. A comparative temperature control with an external thermal element revealed that the accuracy of the high-temperature oven varied between 5 and 10 °C.
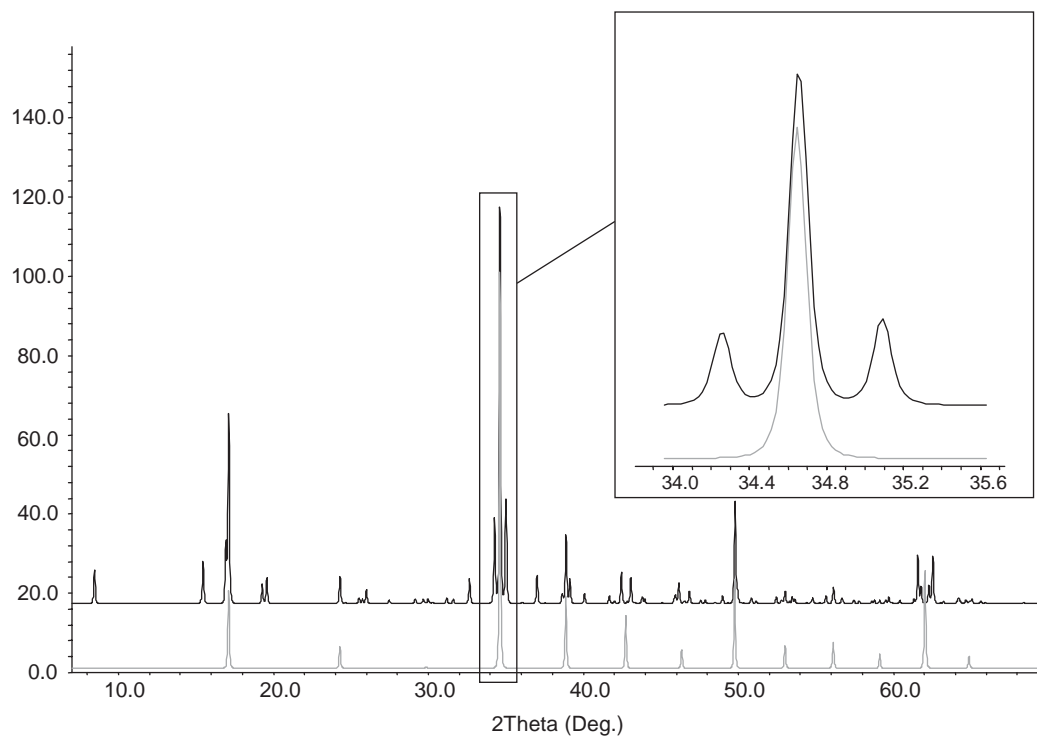
Fig. 2. Simulated powder patterns of α-Ca$_3$(BN$_2$)$_2$ (*Im$\overline{3}$m*, bottom), and β-Ca$_3$(BN$_2$)$_2$ (*Cmca*, top). The zoomed detail shows the selected 2θ range for the temperature-dependent measurements. The displayed section of the calculated pattern represents α-Ca$_3$(BN$_2$)$_2$ with the 2 2 0 reflection, and the calculated pattern of β-Ca$_3$(BN$_2$)$_2$ with 8 0 0, 2 2 4, and 4 0 0 reflections.
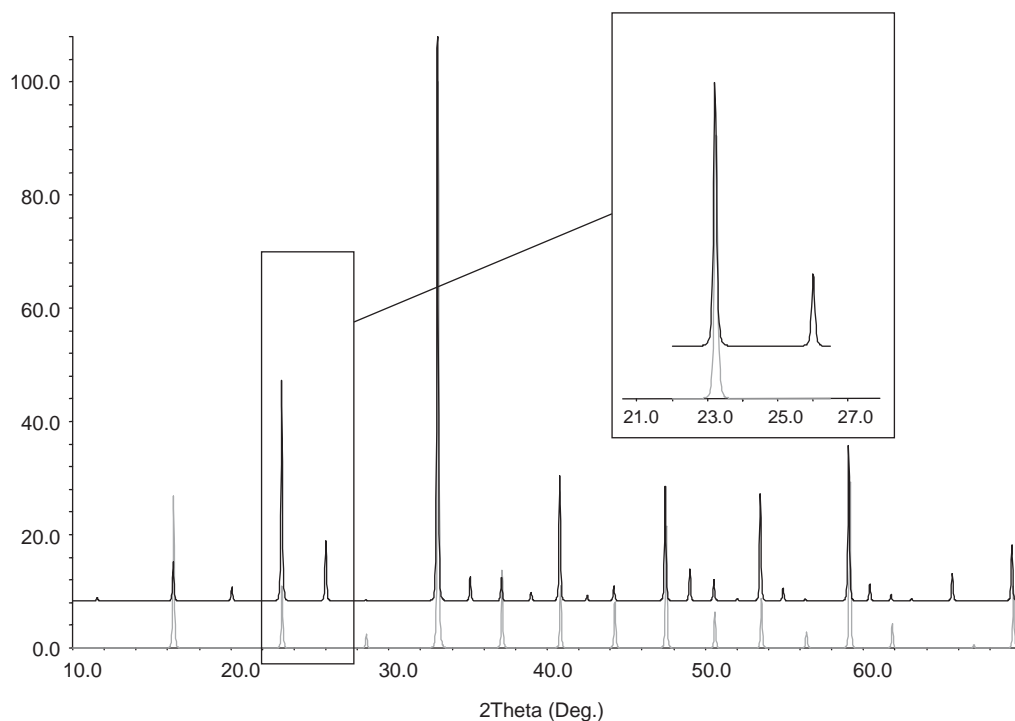
Fig. 3. Simulated powder patterns of α-Sr$_3$(BN$_2$)$_2$ (*Im$\overline{3}$m*, bottom), and β-Sr$_3$(BN$_2$)$_2$ (*Pm$\overline{3}$m*, top). The zoomed detail shows the selected 2θ range for the temperature-dependent measurements, and displays a section of the calculated pattern of α-Sr$_3$(BN$_2$)$_2$ with the 2 0 0 reflection and calculated pattern of β-Sr$_3$(BN$_2$)$_2$ with 2 0 0 and 2 1 0 reflections.

2.3. DSC measurements

The samples were studied by differential scanning calorimetry (DSC) using a Netzsch simultaneous thermal analysis apparatus (STA 409). Measurements were performed in Cu–Au vessels in a continuous N_2 flow. The heating rates were varied between 5 and $10\,^\circ$C/min.

3. Results and discussion

3.1. A structural model for β-Ca$_3$(BN$_2$)$_2$

The powder pattern of β-Ca$_3$(BN$_2$)$_2$ was indexed in a C-centred orthorhombic cell ($a = 1024.18(2)$ pm, $b = 732.43(2)$ pm, and $c = 2091.60(4)$ pm) using the program WinXPow [11] with possible space groups $C2cb$ (No. 41) and $Cmca$ (No. 64).

The crystal structure of β-Ca$_3$(BN$_2$)$_2$ was solved and refined using the programs EXPO and Fullprof [12,13]. Calculations in space group $Cmca$ (No. 64) resulted in the best solution (Table 3). Comparison between the calculated and measured powder patterns is shown in Fig. 4. Final structure refinements yielded satisfactory results for the refined atom positions and reliability factors. But the presence of some side phases, and the relative large number of refinement parameters leads to poor overall isotropic-equivalent displacement parameters for some boron atoms (Table 4).

The orthorhombic structure of β-Ca$_3$(BN$_2$)$_2$ contains three crystallographically distinct BN_2^{3-} units. The environment of the $(BN_2)^{3-}$ units is altered as a result of the vacancy ordering. In contrast to the structure of α-Ca$_3$(BN$_2$)$_2$ in which each N atom of the unit has five Ca neighbours generating a square pyramidal environ-

Table 3
Results of the Rietveld refinement on β-Ca$_3$(BN$_2$)$_2$

Formula	Ca$_3$(BN$_2$)$_2$
Z	12
Molar mass	173,07 g/mol
Temperature	298 K
Wavelength	1,54060 pm
Crystal system	Orthorhombic
Space group	$Cmca$
Cell parameter	$a = 1024,18(2)$ pm, $b = 732,43(2)$ pm, $c = 2091,60(4)$ pm
Angular range	$5^\circ \leqslant 2\theta \leqslant 130^\circ$
Number of independent reflections	238
Number of refined structural parameters	36
R_{Bragg}	7.14%
R_{wp}	9.05%
R_p	6.78%
χ^2	1.85

ment, in β-Ca$_3$(BN$_2$)$_2$ only the N atoms of one $(BN_2)^{3-}$ unit have this type of environment. In the second $(BN_2)^{3-}$ unit only one N atom has five Ca neighbours generating a square pyramidal environment and the other N has only four Ca neighbours, leading to a distorted tetrahedral environment. In the third $(BN_2)^{3-}$ unit both N atoms have only four Ca neighbours generating a distorted tetrahedron.

The presence of three distinct $(BN_2)^{3-}$ ions in the structure of β-Ca$_3$(BN$_2$)$_2$ was confirmed by vibration spectroscopy. The Raman spectrum shows three bands at 1075, 1083, and 1091 cm^{-1} which can be assigned as symmetric stretching modes v_1(B–N) of the three different sets of di-nitridoborate groups [14].

3.2. Symmetry considerations

The super-structure of β-Ca$_3$(BN$_2$)$_2$ is a result of the ordering of ions and vacancies on the $8c$ position of the cubic α-Ca$_3$(BN$_2$)$_2$ structure. The lattice parameters of orthorhombic β-Ca$_3$(BN$_2$)$_2$ are $a_o = 1024.18(2)$, $b_o = 732.43(2)$ and $c_o = 2091.60(4)$ pm and the unit cell can be related with the cubic cell parameter ($a_c = 732.24(3)$ pm) by $a_o \approx \sqrt{2}a_c$, $b_o \approx \sqrt{2}a_c$, and $c_o \approx 2\sqrt{2}a_c$. The structural relation between the refined crystal structure of β-Ca$_3$(BN$_2$)$_2$ and α-Ca$_3$(BN$_2$)$_2$ is displayed in Fig. 5. It can be seen that the cubic and the orthorhombic structures can be well related to each other, and that the differences in both structures are due to the cation ordering.

In order to correlate the two Ca$_3$(BN$_2$)$_2$ phases with each other in terms of symmetry and atom positions, the space group $Cmca$ (No. 64) was generated as a subgroup of $Im\bar{3}m$ with an index of 24 [15,16]. This, and all *translationengleiche* (t) and *klassengleiche* (k) transitions, origin shifts, and the transformation of the lattice parameters are presented in Fig. 6. Corresponding atomic positions were derived all along the symmetry reduction for each step, and the resulting space group ($Cmca$) as well as the derived general atom positions match with the results from the X-ray structure refinement [17].

3.3. Phase transition studies on Ca$_3$(BN$_2$)$_2$

Phase transitions between the low (β) and the high-temperature (α) forms of Ca$_3$(BN$_2$)$_2$ were studied by temperature-dependent DSC and in situ X-ray diffraction.

When β-Ca$_3$(BN$_2$)$_2$ was heated from room temperature a distinct endothermic process was observed in the DSC curve at about $250\,^\circ$C (onset point approx. $240\,^\circ$C) indicating a phase change into α-Ca$_3$(BN$_2$)$_2$ (Fig. 7). Upon cooling, a small exothermic process is observed near $208\,^\circ$C (onset point approx. $225\,^\circ$C) indicating the transformation into the low-temperature phase. PXRD
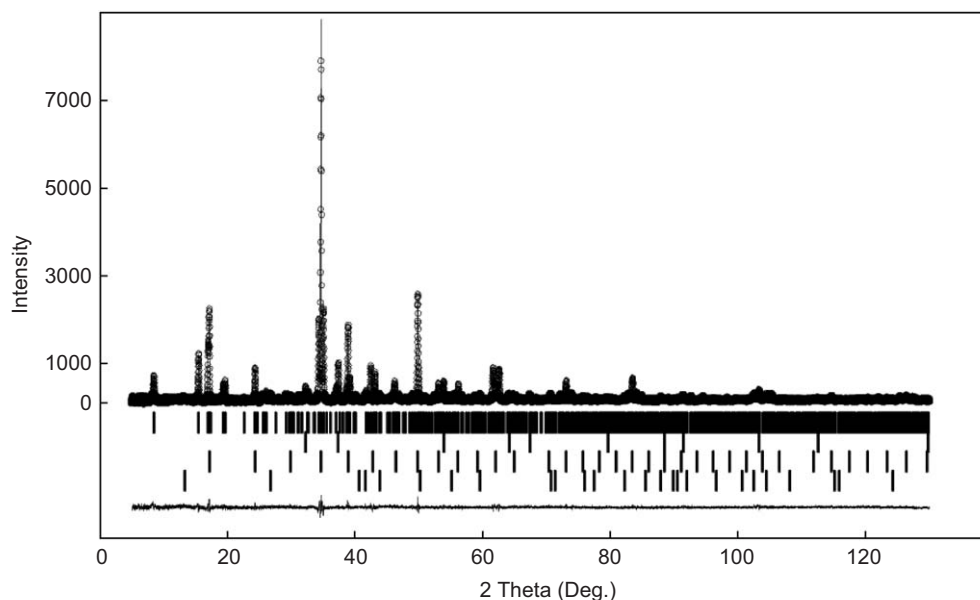
Fig. 4. Measured and calculated powder patterns of β-$Ca_3(BN_2)_2$ with the difference plot after the Rietveld refinement and Bragg positions (top to bottom: β-$Ca_3(BN_2)_2$, BN, α-$Ca_3(BN_2)_2$ and CaO).

Table 4
Atomic coordinates and isotropic-equivalent displacement parameters ($\mathring{A}^2$) for α-$Ca_3(BN_2)_2$

Atom	Wyckoff-pos.	x	y	z	B_{iso} (in $pm^2 \times 10^4$)
Ca1	8f	1/2	0.0303(8)	0.7539(2)	0.9(1)
Ca2	8f	0	0.2588(6)	0.8773(4)	0.62(9)
Ca3	16g	0.7455(2)	0.5200(5)	0.8775(1)	1.21(8)
Ca4	4b	0	1/2	0	1.2(2)
Ca4a	4a	0	0	0	1.2(2)
B1	8e	3/4	0.281(4)	3/4	3.0(8)
B2	8f	1/2	0.263(3)	0.883(1)	0.2(5)
B3	8c	3/4	1/4	0	−0.5(5)
N1	8f	1/2	0.446(2)	0.8554(5)	1.7(4)
N2	16g	0.6774(8)	0.791(1)	0.9482(4)	1.0(3)
N3	16g	0.6575(7)	0.281(1)	0.7043(4)	0.3(2)
N4	8f	1/2	0.085(1)	0.8758(8)	0.5(3)

pattern of the resulting material showed the expected reflections of β-$Ca_3(BN_2)_2$ at room temperature. The pronounced endothermic effect is a hint that the transformation may be a first-order transition. Unfortunately, it was impossible to freeze the high-temperature modification due to the low (natural) cooling rate of the DSC oven.

X-ray diffraction studies were performed to understand the structural changes that occur during the cycling behaviour between the two $Ca_3(BN_2)_2$ phases. The selected 2θ range (between $34°$ and $35.5°$) includes the cubic 2 2 0 reflection of α-$Ca_3(BN_2)_2$. Almost superposed is the orthorhombic 2 2 4 reflection that is flanked by the orthorhombic reflections 8 0 0 and 4 0 0 of β-$Ca_3(BN_2)_2$.

A set of temperature-dependent X-ray measurements in the temperature interval between 180 and 250 °C (with heating and cooling rates of 10 °C/min) were performed to gather more detailed information near the transition temperature. A cyclic heating–cooling procedure starting and ending with β-$Ca_3(BN_2)_2$ is shown in Fig. 8. The $\beta \rightarrow \alpha$ transformation was found to be complete at 230 °C, the back transformation $\alpha \rightarrow \beta$ began between 220 and 210 °C. The results of the temperature-dependent PXRD and DSC measurements agree within the accuracy of the equipments.

In situ temperature-dependent XRD studies allowed us to control phase transitions under different heating and cooling rates (10–50 °C/min) between room temperature and 250 °C, and to freeze the high-temperature
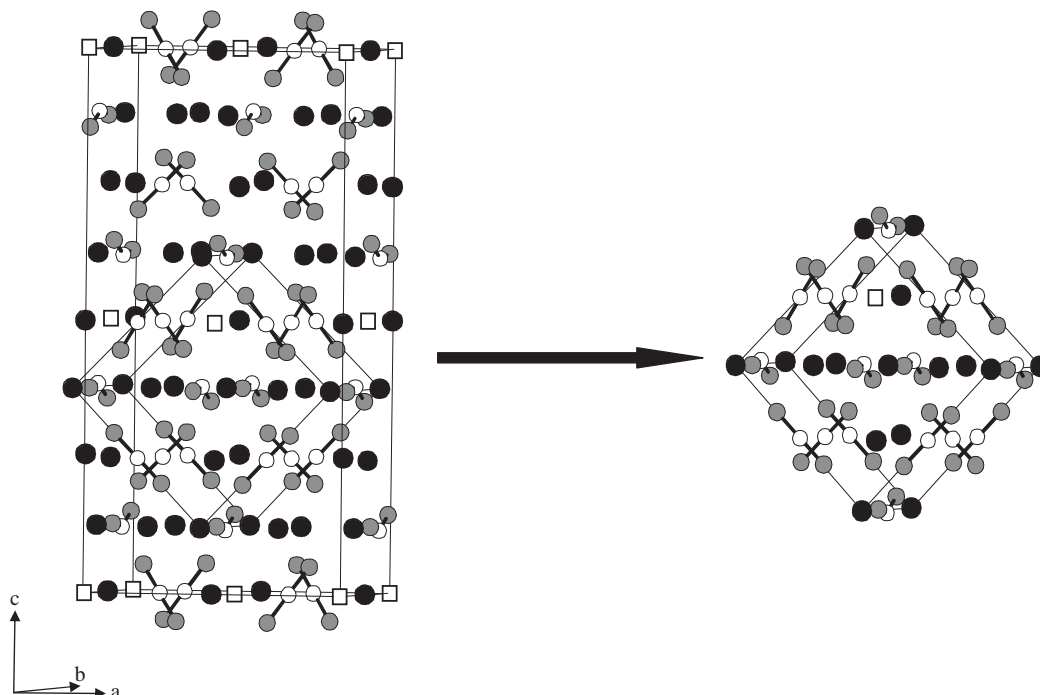
Fig. 5. Unit cell of β-Ca$_3$(BN$_2$)$_2$ (left) and the unplugged pseudo-cubic fragment corresponding to the high-temperature modification. Cation vacancies are indicated by squares.
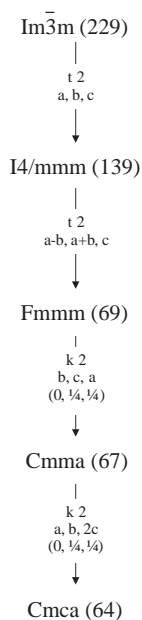

Fig. 6. Group–subgroup relation from the space group $Im\bar{3}m$ to $Cmca$, with transition type (t = translationengleich, k = klassengleich) and order, cell-transformation, and (origin shift) of the lattice parameters.

phase. The experiments started with the reversible $\beta \rightarrow \alpha \rightarrow \beta$ transformation for Ca$_3$(BN$_2$)$_2$ shown in Fig. 9, as observed in the DSC measurement. The occurrence of the high-temperature phase α-Ca$_3$(BN$_2$)$_2$ was clearly

indicated by the observation of its 2 2 0 reflection at 250 °C. α-Ca$_3$(BN$_2$)$_2$ was obtained at room temperature, as shown in Fig. 9 when samples were cooled at a cooling rate of approximately 50 °C/min, in accord with previously reported results, suggesting that a cooling rate higher than 30 °C/min was needed in order to freeze α-Ca$_3$(BN$_2$)$_2$ [6].

Both measurements show a hysteresis behaviour. This, and the abrupt extinction of the characteristic reflections of the β-phase indicate a first-order transition for Ca$_3$(BN$_2$)$_2$.

3.4. Phase transition studies on Sr$_3$(BN$_2$)$_2$

Two closely related crystal structures have been reported for Sr$_3$(BN$_2$)$_2$ with the space groups $Pm\bar{3}m$ and $Im\bar{3}m$. The low-temperature modification (β-Sr$_3$(BN$_2$)$_2$, $Pm\bar{3}m$) displayed in Fig. 1(c) was prepared to investigate possible transitions between the primitive and body-centred structures. Temperature-dependent X-ray measurements were performed with 20 °C increments in the temperature interval between 760 and 820 °C (heating and cooling rates varied between 10 and 50 °C/min). The results of these studies are shown in the powder pattern for the 2θ interval between 22.0° and 26.5° in Fig. 10. The cubic 2 0 0 and 2 1 0 reflections belong to the primitive β-Sr$_3$(BN$_2$)$_2$. Upon heating the sample it became clear that the 2 1 0 reflection disappears above 820 °C. This observation is consistent
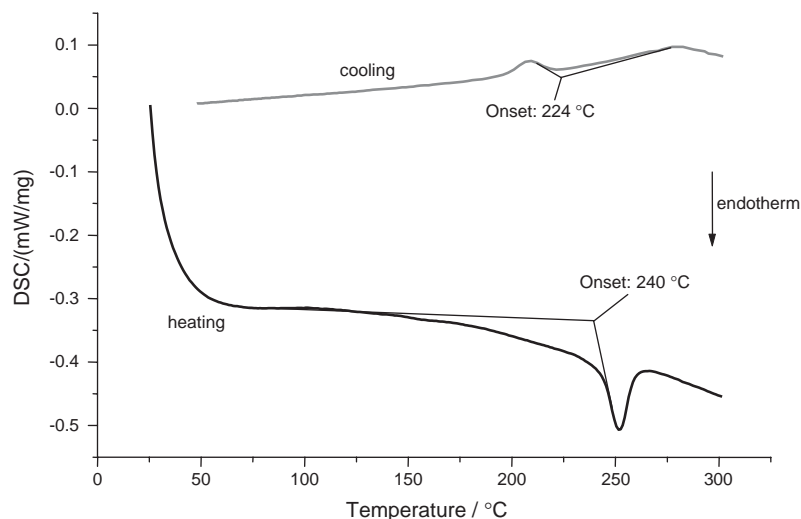
Fig. 7. DSC-measurement of β-Ca$_3$(BN$_2$)$_2$, heating rate 10 °C/min, cooling rate 20 °C/min. On heating, β-Ca$_3$(BN$_2$)$_2$ changes into α-Ca$_3$(BN$_2$)$_2$ at about 240 °C. The back-transformation into α-Ca$_3$(BN$_2$)$_2$ is obtained near 220 °C.
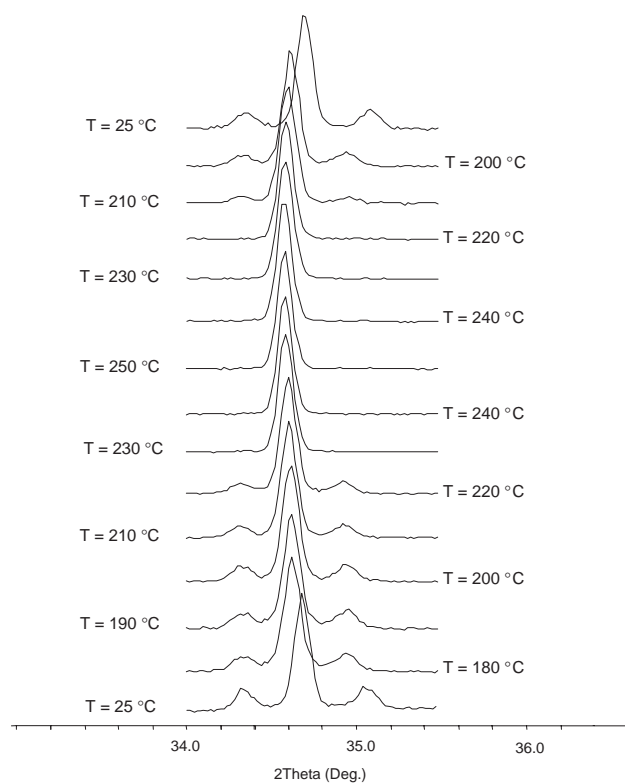
Fig. 8. Powder patterns of Ca$_3$(BN$_2$)$_2$ during heating and cooling between 25 and 250 °C. β-Ca$_3$(BN$_2$)$_2$ is being transformed into α-Ca$_3$(BN$_2$)$_2$ at about 230 °C. The back-transformation into the β-Ca$_3$(BN$_2$)$_2$ cooling is obtained near 210 °C.

Fig. 9. Powder pattern of the transformation between β- and α-Ca$_3$(BN$_2$)$_2$ with different heating and cooling rates. Note the stabilization of the high-temperature modification (α-Ca$_3$(BN$_2$)$_2$) at room temperature through fast cooling (50 °C/min).

with a $\beta \rightarrow \alpha$ phase transition with a transition from a primitive to a body-centred structure, in which the 2 1 0 reflection is systematically absent. This shows that the body-centred cubic structure for Sr$_3$(BN$_2$)$_2$ is the high-
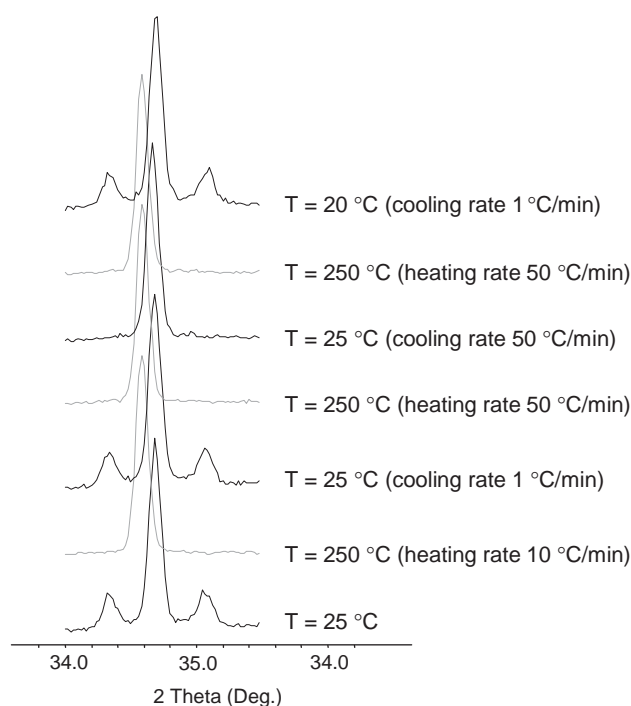
temperature modification. Attempts to isolate α-Sr$_3$(BN$_2$)$_2$ at room temperature with the use of cooling rates up to 50 °C/min failed.

The transition from $Pm\overline{3}m$ to $Im\overline{3}m$ shows a Landau and Lifshiz factors of zero, so that a second-order transition could be possible [16]. In contrast to
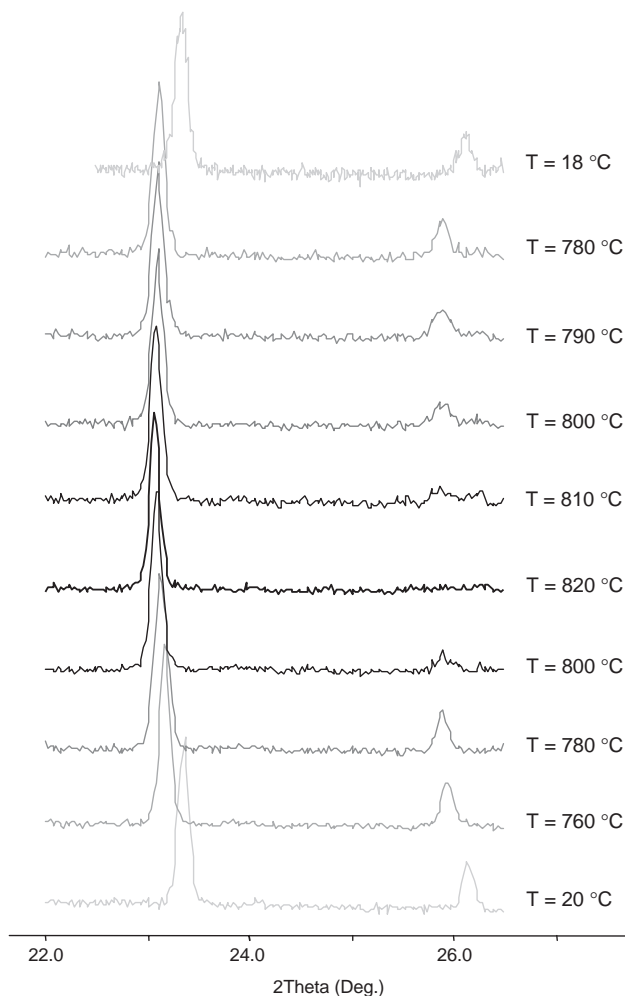
Fig. 10. Powder patterns of β-Sr$_3$(BN$_2$)$_2$ on heating and cooling. The characteristic 2 1 0 reflection of the primitive cell disappears above 820 °C and indicates the transformation into the high-temperature modification. This process is reversed on cooling.

Ca$_3$(BN$_2$)$_2$ there is no hysteresis obtained for the phase transition of Sr$_3$(BN$_2$)$_2$.

4. Conclusion

This investigations has confirmed some former assumptions and have provided new results on the structures and phase relationships of di-nitridoborate phases with the general formula AE_3(BN2)$_2$ with AE = Ca, Sr.

The studies show the structural relationship between the two phases of Ca$_3$(BN$_2$)$_2$ as expected. The low-temperature modification β-Ca$_3$(BN$_2$)$_2$ can be considered as an ordered super-structure of the α-Ca$_3$(BN$_2$)$_2$ structure. The ordering of calcium ions and vacancies involves only a next neighbour ordering distance of $a_c/2$, at a relatively low ordering temperature around

215–240 °C. The phase transition involves a hysteresis and can be regarded as first-order transition according to Stokes and Hatch [16]. The Landau factor is 1 for the first group–subgroup change from $Im\bar{3}m$ to $I4/mmm$. Space group theory also provides an explanation why we were not able to obtain single crystals of β-Ca$_3$(BN$_2$)$_2$. The crystals twin twice because there are the two *translationengleiche* transitions from $Im\bar{3}m$ to $I4/mmm$, and further to $Fmmm$.

The investigations answered the question whether Sr$_3$(BN$_2$)$_2$ crystallizes in the space group $Im\bar{3}m$ or $Pm\bar{3}m$: Both space groups are correct. The high-temperature modification crystallizes in $Im\bar{3}m$ like α-Ca$_3$(BN$_2$)$_2$, while the low-temperature modification crystallizes in $Pm\bar{3}m$. The phase transition involves an ordering of strontium ions from a (disordered) body-centred to a primitive cubic unit cell, with next neighbour ordering distances of strontium ions at $a_c = \sqrt{3/2}a_c$. The fact that the diffusion channels for the strontium ions are tighter and longer may explain the higher transition temperature for Sr$_3$(BN$_2$)$_2$ phases, compared with the Ca$_3$(BN$_2$)$_2$ system. No hysteresis was observed for the phase transition of Sr$_3$(BN$_2$)$_2$.

We have previously stated that α-Ca$_3$(BN$_2$)$_2$ and α-Sr$_3$(BN$_2$)$_2$ are isotypic, which may be safe due to the ample definition of the identifier "isotypic". In spite of the same space group $Im\bar{3}m$, the structures of the α-phases differ in the type of cation disorder. While the $8c$ position is occupied by $\frac{7}{8}$ in α-Ca$_3$(BN$_2$)$_2$ leading to Ca$_2$[Ca$_7$](BN$_2$)$_6$, the position $2a$ is half occupied in α-Sr$_3$(BN$_2$)$_2$ leading to Sr[Sr$_8$](BN$_2$)$_6$. This finding may be explained by the fact that the smaller calcium ions tend to fully occupy the lower coordination $2a$ sites (CN = 6), while larger strontium ions tend to fully occupy the higher coordinated $8c$ sites (CN = 6 + 2).

The cation disorder present in high-temperature phases has a directing effect on structures and symmetries of the corresponding low-temperature phases. When the calcium ions order on $8c$ positions (α-Ca$_3$(BN$_2$)$_2$), the cubic symmetry can no longer exist, and a transition into an orthorhombic structure is observed. In contrast, the cubic symmetry is retained upon the ordering of strontium ions on $2a$ positions (α-Sr$_3$(BN$_2$)$_2$), but a transition into a primitive lattice is obtained (with the position 0,0,0 occupied, and the position $\frac{1}{2},\frac{1}{2},\frac{1}{2}$ empty). Oppositely spoken, the occurrence of the two distinct low-temperature phases supports the assumptions made for the cation disorder in their corresponding high-temperature phases.

α-Ca$_3$(BN$_2$)$_2$ was successfully isolated with a fast cooling rate, and thus stabilized at room temperature. However, it has been reported that traces of carbon can also stabilize α-Ca$_3$(BN$_2$)$_2$ [6]. The same effect could account for the successful preparation of single crystals of α-Sr$_3$(BN$_2$)$_2$ [3]. Unfortunately, it was not possible to

undertake further detailed studies on α-$Sr_3(BN_2)_2$ to better understand the order of its phase transition due to the reactivity of strontium ions with silica near the transition temperature.

Acknowledgments

References

[1] J. Goubeau, W. Anselment, Z. Anorg. Allg. Chem. 310 (1961) 248.

[2] H. Yamane, S. Kikkawa, M. Koizumi, J. Solid State Chem. 71 (1987) 1.

[3] H. Womelsdorf, H.-J. Meyer, Z. Anorg. Allg. Chem. 620 (1994) 265.

[4] M. Somer, U. Herterich, J. Čurda, W. Cabrillo-Cabrera, A. Zürn, K. Peters, H.G. von Schnering, Z. Anorg. Allg. Chem. 626 (2000) 625.

[5] M. Häberlen, J. Glaser, H.-J. Meyer, Z. Anorg. Allg. Chem. 628 (2002) 2169.

[6] M. Wörle, H. Meyer zu Altenschilde, R. Nesper, J. Alloys Compds. 264 (1998) 107.

[7] F. Rohrer, Dissertation, Zürich, 1997.

[8] O. Reckeweg, Dissertation, Tübingen, 1998.

[9] O. Reckeweg, F. DiSalvo, M. Somer, J. Alloys Compds. 361 (2003) 102.

[10] M. Somer, C. Gül, R. Müllmann, B.D. Mosel, R.K. Kremer, R. Pöttgen, Z. Anorg. Allg. Chem. 630 (2004) 389.

[11] STOE, WinXPow, Version 1.08., Darmstadt, 2001.

[12] A. Altomare, M.C. Burla, M. Camalli, B. Carrozzini, G.L. Cascarano, C. Giacovazzo, A.G.G. Moliterni, G. Polidori, R. Rizzi, J. Appl. Crystallogr. 32 (1999) 339.

[13] T. Roisnel, J. Rodriguez-Carvajal, Materials Science Forum, Proceedings of the Seventh European Powder Diffraction Conference (EPDIC 7), 2000, p. 118.

[14] Somer, private communication.

[15] T. Hahn, International Tables For Crystallography, fourth ed., Kluwer Academic Publishers, Dordrecht, Boston, London, 1995.

[16] H.T. Stokes, D.M. Hatch, Isotropy Subgroups of the 230 Crystallographic Space Groups, World Scientific, Singapore, New Jersey, London, Hong Kong, 1988.

[17] M. Häberlen, Dissertation, Tübingen, 2005, in preparation.